

Polycationic (Mixed) Core–Shell Dendrimers for Binding and Delivery of Inorganic/Organic Substrates

Arjan W. Kleij,^[a] Rob van de Coevering,^[a] Robertus J. M. Klein Gebbink,^[a] Anne-Marie Noordman,^[a] Anthony L. Spek,^[b] and Gerard van Koten*^[a]

Abstract: The convergent synthesis of a series of polycationic aryl ether dendrimers has been accomplished by a convenient procedure involving quantitative quaternarization of aryl(poly)-amine core molecules. The series has been expanded to the preparation of the first polycationic, mixed core–shell dendrimer. All these dendrimers consist of an apolar core with a peripheral ionic layer which is surrounded by a less polar layer of dendritic wedges. These cationic, macromolecular species have been investigated for their ability to form assemblies with (anionic) guest mole-

cules. The results obtained from UV/Vis and NMR spectroscopies, and MALDI-TOF-MS demonstrate that all the cationic sites throughout the dendrimer core are involved in ion pair formation with anionic guests giving predefined guest/host ratios up to 24. The large NMR spectroscopic shifts of resonances correlated with the groupings located in

the core of the dendrimers, together with the relaxation time data indicate that the anionic guests are associated with the cationic core of these dendrimers. The X-ray molecular structure of the octacationic, tetra-arylsilane model derivative $[\text{Si}(\text{C}_6\text{H}_5\{\text{CH}_2\text{NMe}_3\}_{2-3,5})_4]^{8+} \cdot 8\text{I}^-$ shows that the iodide counterions are primarily located near the polycationic sphere. The new polycationic dendrimers have been investigated for their catalytic phase-transfer behavior and substrate delivery over a nanofiltration membrane.

Keywords: dendrimers • nanofiltration • noncovalent interactions • phase-transfer catalysis • polycations

Introduction

Dendritic polymers^[1] with regular and well-defined unimolecular architectures currently attract much interest as soluble supports^[2] or as so-called dendritic boxes or molecular containers.^[3] The micro-environment inside these materials is usually less densely packed compared with the sterically congested outer shell, which enables the encapsulation of (small) organic guests in the dendritic host. The latter offers the possibility to convert these macromolecules into biologically important delivery systems which can release organic guest molecules by means of external stimulus, for example

irradiation or pH changes.^[4] Most of the dendritic containers reported so far use the concept of closing the dendrimer surface in order to be able to keep the guest molecules inside the dendrimer host. In this case, high generation dendrimer species with sufficient loading of peripheral groups are needed for an effective binding of guest molecules inside their cavities. However, up to now, few reports exist on well-defined molecular containers that exhibit flexible binding properties specifically inside its internal cavities which do not depend on the peripheral crowding of the system but solely on the binding properties at the core.^[5a-c]

Here, we focus on this particular aspect by using a different approach of binding guest molecules inside dendritic host systems. Two types of polycationic species^[5d] were designed; the first one is constructed from polyaryl(di)amine core molecules and contains an ionic core shell and a less polar outer shell. The second type is derived from a relatively large, carbosilane dendritic core producing polycationic mixed core–shell dendrimer species with a potentially variable, but with a distinct distance between the core of the molecule and the ionic layer (Figure 1).

These new polycationic dendrimers can potentially be used for the multiple incorporation of anionic guests inside their core or cavities. Both types of cationic dendrimers should be capable of specific binding to a number of different anionic,

[a] Prof. Dr. G. van Koten, A. W. Kleij, R. van de Coevering
Dr. R. J. M. Klein Gebbink, A.-M. Noordman
Debye Institute, Department of Metal-Mediated Synthesis
Utrecht University, Padualaan 8, 3584 CH Utrecht (Netherlands)
Fax: (+31)30-2523615
E-mail: g.vankoten@chem.uu.nl

[b] Prof. Dr. A. L. Spek
Bijvoet Center for Biomolecular Research
Department of Crystal and Structural Chemistry
Utrecht University, Padualaan 8, 3584 CH Utrecht (Netherlands)
E-mail: a.l.spek@chem.uu.nl

Supporting information for this article is available on the WWW under <http://www.wiley-vch.de/home/chemistry/> or from the author.

organic substrates through electrostatic forces^[6] regardless of the steric features on the surface. Moreover, this behavior is likely to be fully reversible, which could be relevant for an eventual reuse of the system. The application of these systems in phase-transfer catalysis and substrate delivery over a nanofiltration membrane is presented.

Results and Discussion

Synthesis of model species: In order to investigate whether arylamine building blocks could be used for the construction of larger (dendritic) macromolecules, we first carried out quaternarization of a model tetra-arylsilane compound, namely $\text{Si}(\text{C}_6\text{H}_3\{\text{CH}_2\text{NMe}_2\}_{2-3,5})_4$ (abbreviated as $\text{Si}(\text{NCN})_4$) (**1a**)^[7] with various alkyl halides. In order to be able to vary the amount of anchoring groups and the final structure of the polycationic products we have also prepared core molecule **1b** (Scheme 1). Core molecules **1a** and **1b** give rise to eight and four ammonium centers, respectively, after quaternarization. Core molecule **1b** was obtained as a white solid by in situ treatment of an excess of $[\text{LiC}_6\text{H}_4(\text{CH}_2\text{NMe}_2)_4]$ with SiCl_4 in Et_2O at -78°C as described earlier for **1a**.^[7]

Treatment of **1a** with an excess of methyl iodide at RT in CH_2Cl_2 led to the immediate precipitation of a white solid material, which was isolated by centrifugation. ^1H NMR spectroscopic analysis performed in D_2O pointed to selective formation of the octatrimethylammonium derivative $[\text{Si}(\text{C}_6\text{H}_3\{\text{CH}_2\text{NMe}_3\}_{2-3,5})_4]^{8+} \cdot 8\text{I}^-$ (**2**) in nearly quantitative

Abstract in Dutch: Dit onderzoek beschrijft een serie polykationische aryether-dendrimeren, die in kwantitatieve opbrengst zijn verkregen door reactie van dendritische benzyl bromides met organosilanen die vier aryl(di)amine substituenten bevatten. Deze dendrimeren zijn opgebouwd uit een polykationische kern en een polaire buitenlaag. Tevens wordt de synthese van het eerste gemengde, polykationische dendri-meer beschreven. Dit nieuwe type dendri-meer bestaat achtereenvolgens uit een [G1] carbosilaandendri-meer kern, een poly-ionische tussenlaag en een polaire buitenlaag opgebouwd uit [G1] Fréchet type dendrons. De bindingscapaciteiten van deze dendrimeren ten aanzien van anionische gast-molekulen zijn onderzocht. Spectroscopische metingen (UV/Vis, NMR en MALDI-TOF) wijzen erop dat alle kationische centra in de dendrimeren beschikbaar zijn voor de vorming van ionparen. Zo is het mogelijk om een maximum aantal van 24 anionische gasten te binden. De grote NMR spectroscopische verschuivingen gecombineerd met relaxatiemetingen van de groepen die aanwezig zijn in de kern van de dendrimeren, duiden op een duidelijke associatie van de anionen met de kationische centra van de dendrimeren. De kristalstructuur van de octakationische model-verbinding $[\text{Si}(\text{C}_6\text{H}_3\{\text{CH}_2\text{NMe}_3\}_{2-3,5})_4]^{8+} \cdot 8\text{I}^-$ laat zien dat de (jodide) anionen zich voornamelijk in de buurt van de kationische centra bevinden. De nieuwe polykationische dendrimeren zijn gebruikt in fase-transfer katalyse en voor het transport van organische substraten door nanofiltratiemembranen.

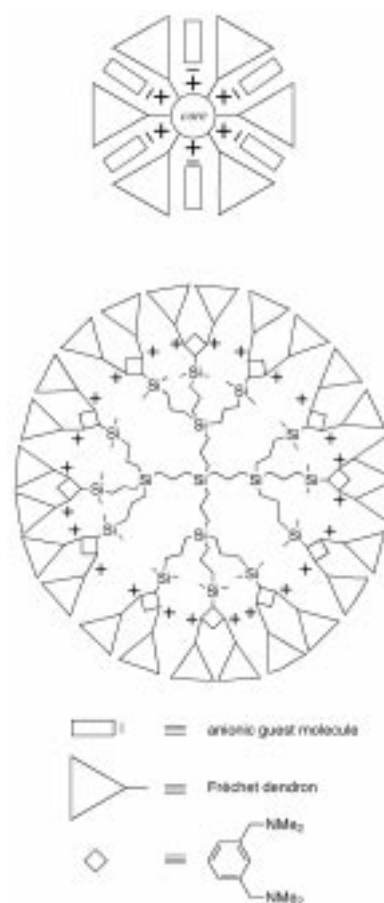
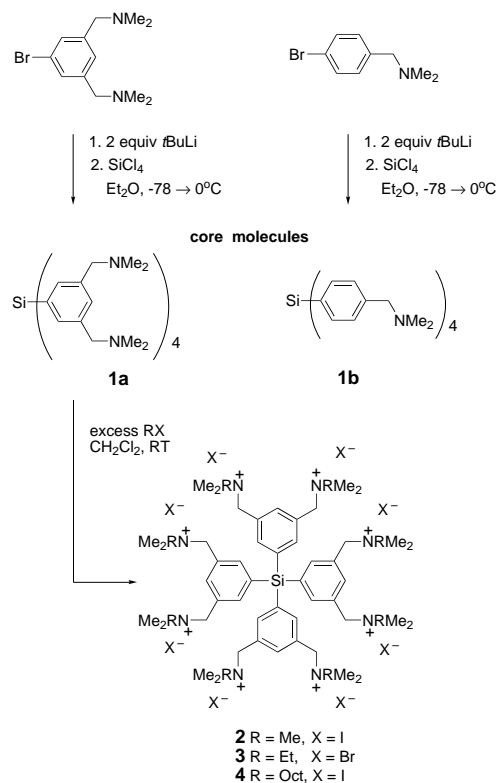


Figure 1. Schematic representation of two types of polycationic macromolecular hosts for anionic guest molecules.



Scheme 1. Synthesis of core molecules **1a** and **1b** and model polycationic species **2–4**.

yield. This procedure proved to be of general use and the octaethyl and octa-octyl derivatives **3** and **4** were also isolated as white solids in good yields by treatment of **1a** with ethyl bromide and octyl iodide, respectively (Scheme 1).

Compounds **2–4** are hygroscopic solids melting between 73–77 °C without decomposition, unlike the polycationic materials prepared by Stoddart et al.^[8] The composition of **2–4** was confirmed by NMR spectroscopy, fast atom bombardment (FAB) mass spectroscopy, and elemental microanalysis. The FAB mass spectra of **2–4** showed characteristic isotopic distributions at m/z 1801.0, 1585.1, and 2587.0, corresponding to $[2 - I]^+$, $[3 - Br]^+$, and $[4 + H - I]^+$, respectively. Beside these easily assignable peaks, the spectra also showed other complicated isotope patterns that most likely resulted from the exchange of halide anions with matrix molecules,^[9a] as well as degradation of the quaternary ammonium salts via C–N bond cleavage.^[10]

The solubility characteristics of these dendritic cationic derivatives varied upon increasing the length of the alkyl halide: Octamethylated **2** is only soluble in H₂O and MeOH whereas the octa-octylated derivative **4** is insoluble in water and dissolves readily in relatively non-polar solvents such as CH₂Cl₂ and CHCl₃. This effect can be rationalized by assuming that the aliphatic octyl chains in **4** strongly interact with each other and thus shield the hydrophilic polycationic core, similar to a reversed micelle. The ¹H NMR spectra recorded for **4** at different concentrations showed more than one set of resonances for the aromatic protons and CH₂N and NMe₂ groupings. Similar dependencies of the NMR spectroscopic patterns on the concentration of dendritic ammonium salts have been reported.^[9b]

X-ray crystal structure of **2**:

Although several groups have characterized organic molecules crystallographically containing triorganoammonium iodide moieties,^[11] the structure of **2** in the solid state is the first example of a polyammonium derivative containing more than four of such groupings within a single molecule. Moreover, this X-ray crystal structure can be regarded as a representative model for the poly-

cationic core of the dendrimer species presented here (see below). Crystals of **2** were obtained from a 2:1 mixture of MeOH/EtOH at –20 °C. The polycationic part of the molecular structure of **2** is depicted in Figure 2, top and relevant bond lengths and angles are given in Table 1. Crystallographic data and other related details are summarized in the Experimental Section.

It should be noted that the refinement of the data was troublesome because of the large disorder of the solvent molecules and partial disorder of the iodide anions. A first impression of the unique solid state structure of octacationic **2** could be obtained emphasizing a fully methylated species with eight quaternarized amine moieties forming a soft, cationic sphere at about 5.9 Å from the centroid Si center. Although partially disordered, the larger part of the iodide anions are primarily located near/between the cationic centers (Figure 2,

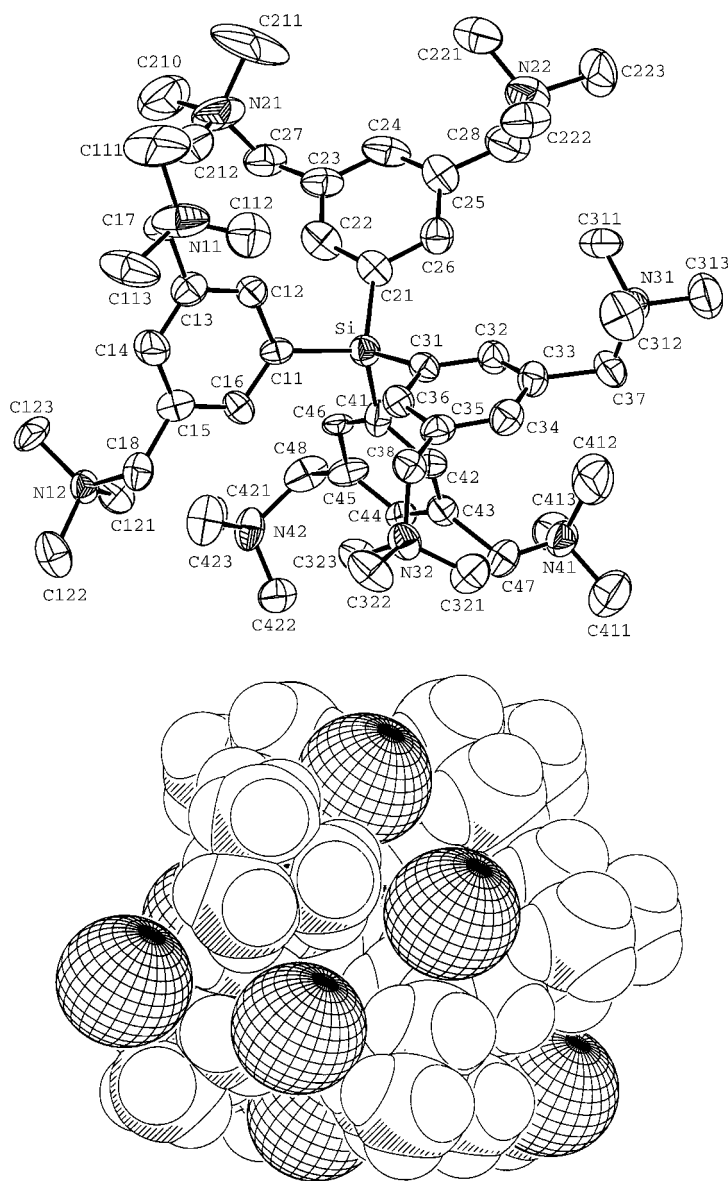


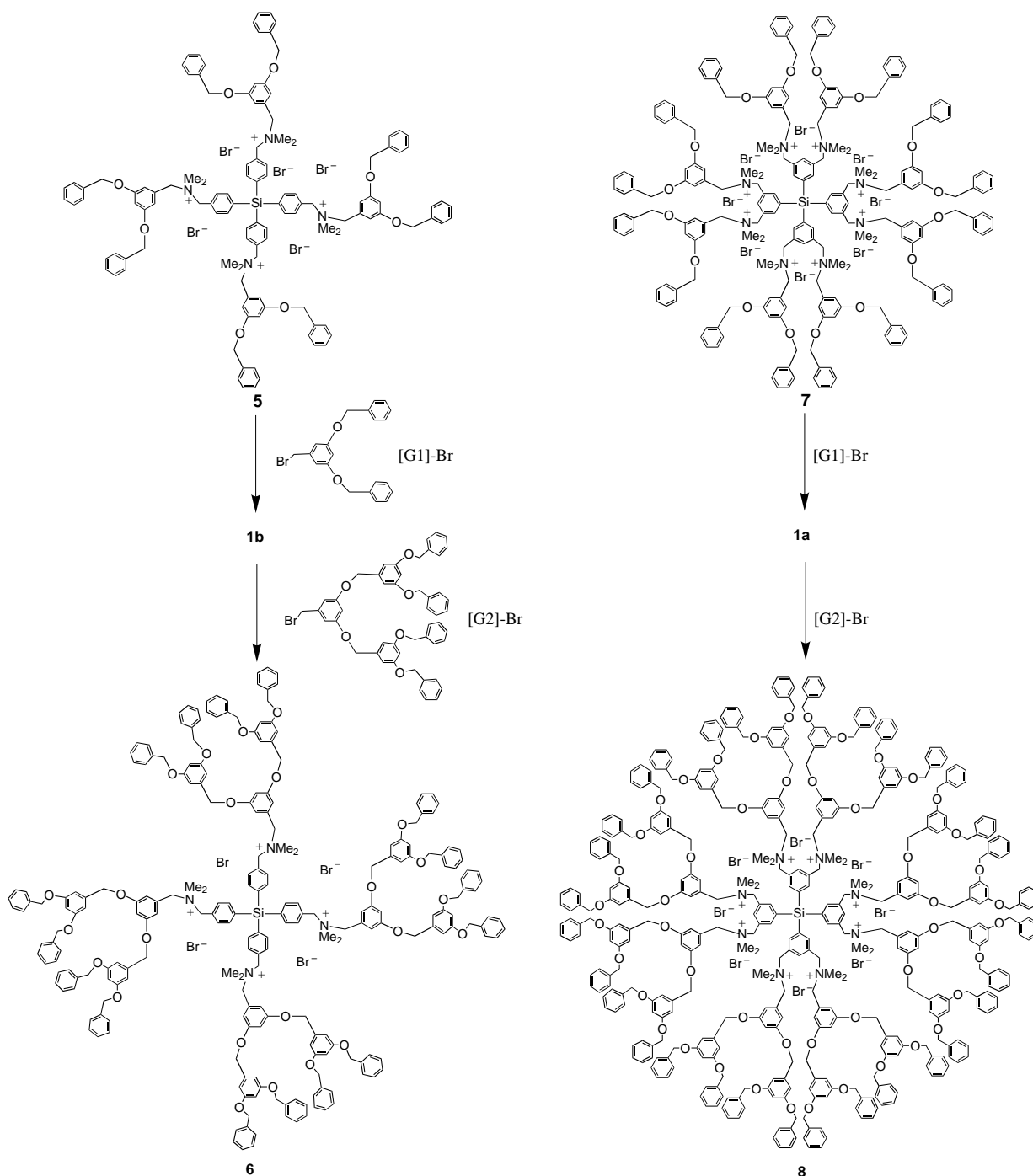
Figure 2. Top: Displacement ellipsoid plot (ORTEP, 50% probability level) of the polycationic part of the molecular structure of **2**. Hydrogen atoms, iodide anions, and cocrystallized, disordered solvent molecules have been omitted for clarity. Bottom: Space-filling model of the molecular structure of the polycationic unit of **2** together with the iodide anions.

Table 1. Selected bond lengths [\AA] and angles [$^\circ$] for **2** with esd's in parentheses.

bond lengths			
Si–C11	1.896(17)	Si–C21	1.878(19)
Si–C31	1.891(18)	Si–C41	1.854(19)
N11–C111	1.60(5)	N12–C121	1.47(2)
N11–C112	1.42(4)	N12–C122	1.53(2)
N11–C113	1.57(3)	N12–C123	1.50(2)
bond angles			
C11–Si–C21	105.7(8)	C11–Si–C31	108.0(7)
C11–Si–C41	111.7(8)	C21–Si–C31	116.4(8)
C21–Si–C41	108.4(8)	C31–Si–C41	106.7(7)

bottom). The presence of the relatively large iodide anions near the cationic core could be responsible for the minor deviations from ideal geometry found for some bond lengths and angles (Table 1). The key point of this structure is that it substantiates earlier implications that anions could be accommodated inside dendritic structures by means of ion pair formation,^[8] though in solution this feature may not be fully retained.

Synthesis of polycationic aryl ether dendrimers: The dendritic molecules **5–8** (Scheme 2) were constructed from the tetra-

Scheme 2. Synthesis of the polycationic dendrimers **5–8**.

arylsilane building blocks **1a** and **1b**, and Fréchet-type dendrons (abbreviated as [G1]-Br or [G2]-Br)^[12a] under mild reaction conditions (CH₂Cl₂, RT). These dendrons contain a benzyl bromide focal point that can be used for the selective and quantitative quaternarization of the nitrogen atoms present in the core molecules **1a** and **1b**.^[12b] This gave almost quantitative yields (95–100%) of the functionalized macromolecules **5–8** as white, hygroscopic solids. These dendrimer species were fully characterized by NMR spectroscopy (¹H and ¹³C{¹H}), electrospray mass spectrometry (ES-MS), and combustion analyses, which confirmed in all cases the isolation of a single product. The ES-MS spectra recorded for **5–8** showed, for example, the presence of multiple cationic fragment ions at *m/z* 969.3 (calcd for [**5**-2Br]²⁺: 969.1), 1818.6 (calcd for [**6**-2Br]²⁺: 1818.1), 1849.8 (calcd for [**7**-2Br]²⁺: 1849.9), and 2338.7 (calcd for [**8**-3Br]³⁺: 2338.5), respectively.

Compounds **5–8** are soluble in solvents such as CH₂Cl₂ and toluene, but are essentially insoluble in water. This behavior strongly suggests that the local, ionic environment inside these dendrimers is well-shielded by the outer, polyether dendrons (cf. the position of the iodide anions in the structure of **2**). Molecular mechanics studies^[13] performed on **7** and **8** supported this assumption and showed that these dendrimers are able to adopt structures in which potential guests can be embedded in the internal cavities (Figure 3).

Preparation and analysis of a mixed core-shell dendrimer species: Beside the preparation of dendrimers with a central ionic core, we have also prepared a polycationic mixed dendrimer species **9** (Scheme 3). The synthesis of **9** was realized by treatment of the known carbosilane dendrimer [G1]-SiMe₂-NCN^[7] with a slight excess of a first generation Fréchet-dendron [G1]-Br as described for the preparation

of **5–8** (see below) to give the new dendrimer species [G1]-SiMe₂-NCN·24[G1]-Br (**9**) as a white solid in quantitative yield. Dendrimer **9** consists of three distinctive layers: a rather apolar carbosilane inner shell, a middle ionic shell, and an less polar outer shell.

¹H and ¹³C{¹H} NMR spectroscopic analysis of this new dendrimer showed that all the tertiary amines had successfully

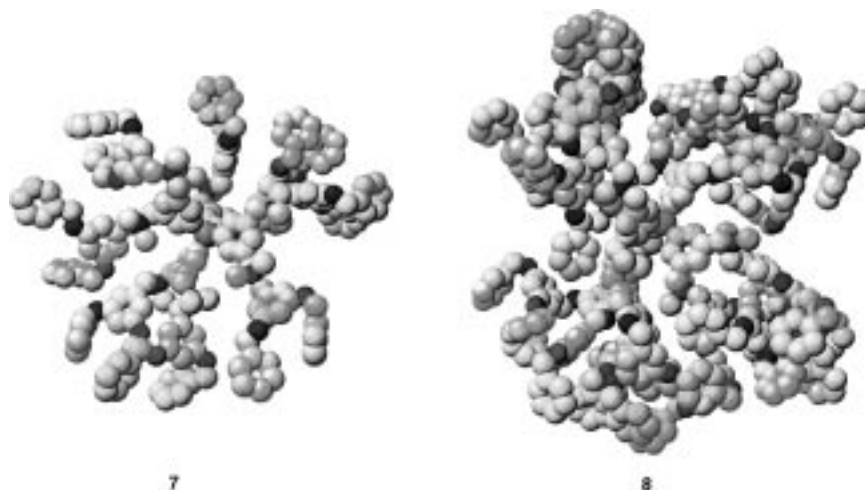
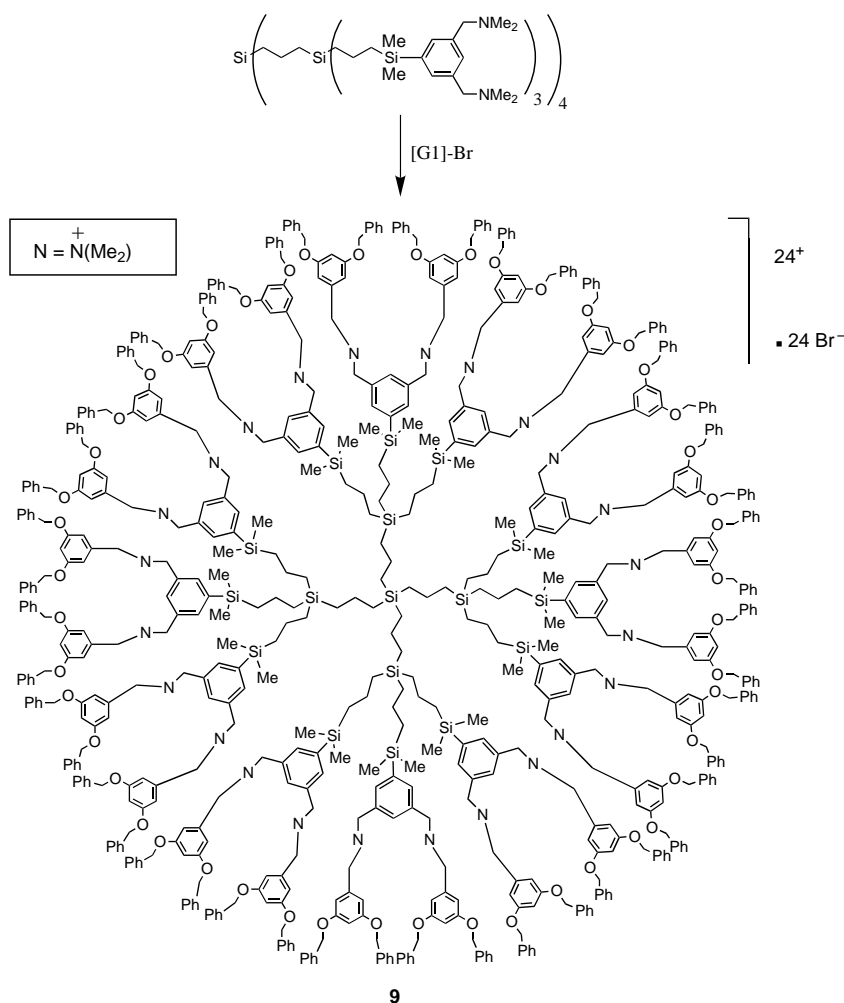


Figure 3. Space-filling models of the calculated energy-minimized polycationic structures of **7** and **8**.



Scheme 3. Synthesis of the mixed dendrimer species **9**.

been quaternized with [G1]-Br Fréchet dendrons. The $^{29}\text{Si}\{^1\text{H}\}$ NMR spectrum recorded for **9** showed only two distinctive broad peaks at $\delta=0.77$ and -2.07 . The resonances corresponding to the central silicon and those for the inner layer of silicon nuclei, most probably coincide at $\delta=0.77$. The increase in broadness of the Si resonances is indicative of a decrease in molecular motion upon introduction of [G1] dendrons. The structure of **9** was further supported by elemental analysis and ES-MS. The ES mass spectrum recorded for **9** displayed distinctive peaks at m/z 3171.4 (calcd for $[\mathbf{9}-4\text{Br}]^{4+}$: 3171.7), 2521.5 (calcd for $[\mathbf{9}-5\text{Br}]^{5+}$: 2521.3), and 2088.0 (calcd for $[\mathbf{9}-6\text{Br}]^{6+}$: 2087.8).

Preparation and analysis of host–guest systems: We decided to investigate the exchange of the bromide anions in **5–9** for anionic organic molecules. In a model study, the CH_2Cl_2 -insoluble dye methyl orange (abbreviated as MO) was selected as a diagnostic probe for spectroscopic analysis. The set-up for the anion exchange in the various polycationic dendrimers is outlined in Figure 4. In a two-phase layer system (Figure 4A), stoichiometric amounts of MO were dissolved in water (orange color) along with one of the polycationic dendrimers **5–9** in CH_2Cl_2 (colorless). Thorough mixing of the two layers gave rise to almost instantaneous decolorization of the water layer and concomitant colorization of the organic phase; this indicated the exchange of bromide for MO anions. These two-phase mixtures can be stored for months without any observable colorization of the water layer. The precise mechanism of formation of these dye–dendrimer assemblies is not known. It has been postulated that similar phase-transfer processes are accompanied by diffusion of water into the dendrimer core.^[3b] The dye–dendrimer assemblies were studied by UV/Vis spectroscopy (residual amount of MO in the water layer), ^1H NMR spectroscopy, and MALDI-TOF mass spectrometry (CH_2Cl_2 layer). From the spectroscopic investigations, the number of MO molecules present in the dendrimer could be quantified (Table 2). The spectroscopic analyses pointed to a full exchange of bromide for MO anions and, therefore, suggest that all ammonium cations in the dendritic hosts are available for the formation of dye–dendrimer assemblies. It should be noted that the use of both a stoichiometric amount and an excess of MO in the two-phase system (Figure 4) leads to quantitative exchange of bromide for MO anions in the dendrimer species **5–8**. Another interesting aspect is that the number of guests could easily be regulated and monitored. The addition of less than the stoichiometric

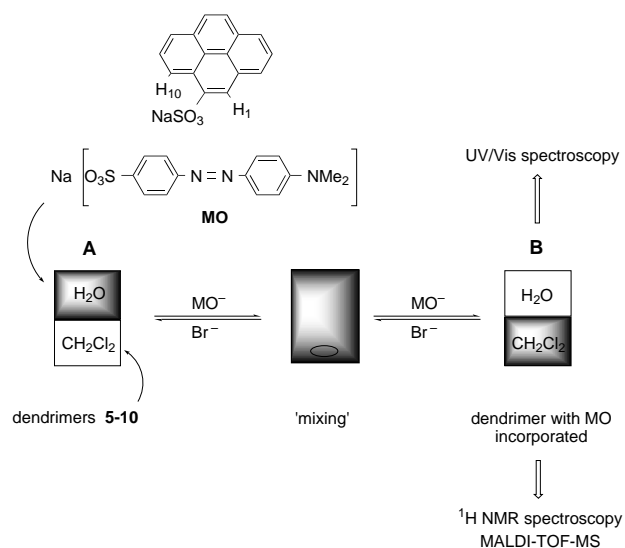


Figure 4. Set-up for the assembly of inorganic/organic anions with the polycationic dendrimer species **5–10**.

amount (1–3 equiv) of MO with respect to the number of cations present in dendrimer **5**, led to the assembly of one, two, or three MO anions with the cationic dendrimer, respectively, as was easily recognized in the ^1H NMR spectra by the increase in intensity of new resonances at $\delta=8.02$, 7.78, 7.69, and 6.68 (all doublets, ArH) and 3.02 (singlet, NMe_2 group) that were attributed to MO guest anions. The ^1H NMR spectra of these MO-containing species showed a stepwise increase in $\Delta\delta$ for the NMe_2 groups of the cationic core unit in **5** upon binding more MO anions, which allowed the (further) NMR spectroscopic assignment.

It should be mentioned that the assembly of MO with the polycationic dendrimeric structures **5–8** is fully reversible. The addition of an excess of bromide anions to the water phase completely decolorized the organic layer and, simultaneously, colorized the water phase. The dye anions could also be liberated by lowering the pH of the mixture. This gave rise to the formation of the corresponding acid of MO, which is soluble in both the organic as well as the water phase.

The dye–dendrimer assemblies **5·4MO**, **6·4MO**, **7·8MO**, **8·8MO**, and **9·24MO** were isolated as bright orange solids, which are soluble in CH_2Cl_2 , THF, and benzene similar to the bromide-containing, polycationic dendrimers.^[14] The NMR spectra of these MO-containing species proved to be very illustrative. The resonances assigned to the dendrimer core were broadened, while the signal belonging to the NMe_2 grouping of MO was found as a relatively sharp resonance. Additionally, for the dendrimer core unit typical upfield shifts were found for the NMe_2 grouping, while downfield shifts were observed for the ArH of the core unit (Table 3 and Figure 5, Supporting Information).^[15]

The line-broadening in the ^1H NMR spectra of **5–8** and the corresponding MO assemblies was further qualitatively analyzed by performing spin-lattice (T_1) and spin–spin (T_2) relaxation measurements.^[16] The T_1 relaxation times for several groups (especially the ArH and NMe_2 groups of the core unit) showed a steady increase with increasing molecular weight, that is from **5** to **6** and from **7** to **8** (see also Supporting

Table 2. The number of MO molecules incorporated into the dendrimers **5–9** and **10** determined by ^1H NMR and UV/Vis spectroscopy.

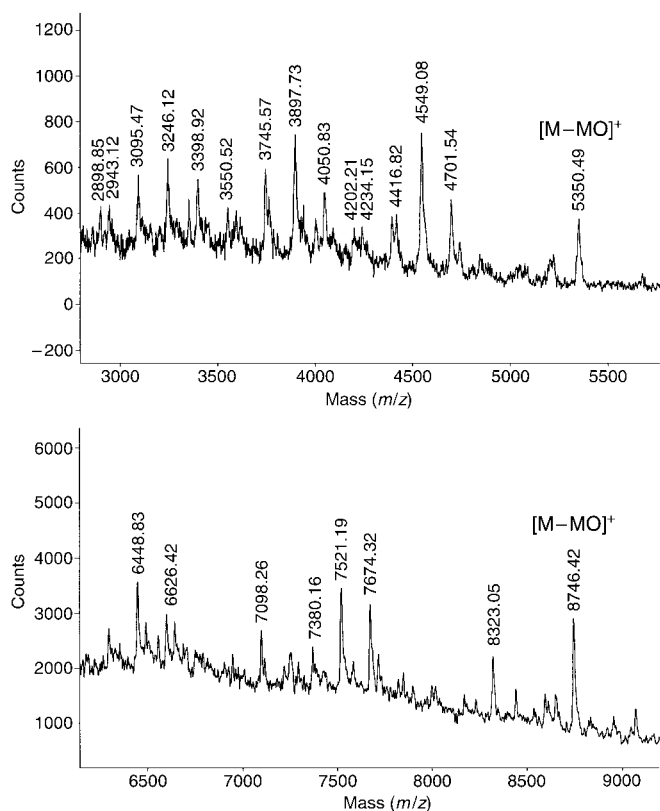
Dendrimer	^1H NMR	UV
5	4.1	4.0
6	4.0	3.5
7	8.2 ^[a]	8.0
8	7.5 ^[a]	8.0
9	23.7	n.d. ^[b]
10	4.0	n.d. ^[b]

[a] Integration less accurate because of line broadening. [b] Not determined.

Table 3. Selected ^1H NMR spectroscopic data for the core resonances of the dendrimers **5–10** and their MO-containing derivatives in CDCl_3 at RT.^[a]

Compound	Cationic sites	ArH	NMe_2
5	4	$\text{Si}[\text{C}_6\text{H}_4(\text{CH}_2\text{NMe}_2^+)_{2-4}]_4\text{-core}$	2.98
		7.77 (d)	2.83
5·4MO		— ^[b]	2.83
6	4		2.97
		7.76 (br)	2.88
6·4MO		— ^[b]	2.88
7	8	$\text{Si}[\text{C}_6\text{H}_3(\text{CH}_2\text{NMe}_2^+)_{2-3,5}]_4\text{-core}$	3.07
		8.41, 8.19	2.78
7·8MO		8.88, 8.75	3.00
8	8		2.81
		8.35, 8.75 (br)	2.81
8·8MO		8.92, 8.72 (br)	2.81
9	24	$[\text{G}1]-[\text{C}_6\text{H}_3(\text{CH}_2\text{NMe}_2^+)_{2-3,5}]_{12}\text{-core}^{[c]}$	3.06
		8.14 (br) ^[d]	2.85
9·24MO		8.10 (br) ^[d]	2.85
10	4	$\text{Me}_2\text{Si}[\text{C}_6\text{H}_3(\text{CH}_2\text{NMe}_2^+)_{2-3,5}]_2\text{-core}$	3.02
		8.35, 8.20	2.92
10·4MO		8.55, 8.37	2.92

[a] All chemical shifts are listed in ppm and signals are singlet resonances unless stated otherwise. Abbreviations used: d = doublet, br = broad signal, MO = methyl orange. [b] The ArH_{core} of these species are coincident with other ArH of the dendrimer. [c] $[\text{G}1] = \text{Si}[(\text{CH}_2)_3\text{Si}[(\text{CH}_2)_3\text{-SiMe}_2\text{-}]_3]_4$. [d] For a possible explanation see ref. [15].

Figure 5. MALDI-TOF-MS spectra recorded for A) **7·8MO** and B) **8·8MO**.

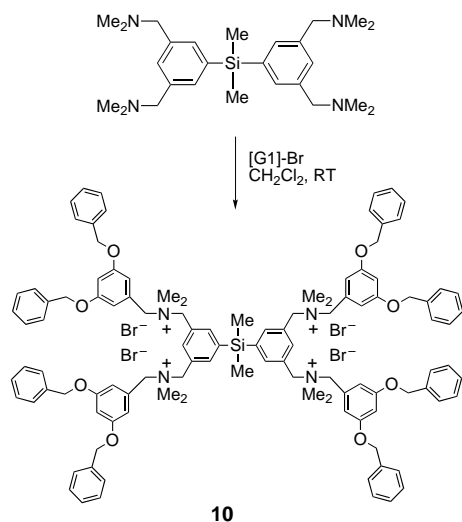
Information). On the other hand, the T_2 relaxation times for the same moieties decreased with higher molecular weights. This has been followed by line shape analysis of the NMe_2 grouping present in the cores of the molecules **5–8**. The ^1H NMR spectra of the MO-containing dendrimer species showed increased overlap between the resonances corre-

sponding to the NMe_2 grouping of the core and the NMe_2 grouping of the MO guest molecules. Nevertheless, an increase in T_1 and further decrease of T_2 was clearly noted when compared with their parent species. These data are in line with earlier reports on relaxation time data measured for dendrimer species.^[3e, 17]

From the latter results, it seems reasonable to assume that the MO anions are associated with the polycationic dendrimers. As a consequence, the dendrimer core unit will be more shielded from the lattice (i.e., solvent) compared with the dendrimers **5–8**, giving rise to the observed higher T_1 and lower T_2 relaxation times. Molecular modeling^[13] has been used to estimate the size of the Fréchet dendrons $[\text{G}1]\text{-Br}$, $[\text{G}2]\text{-Br}$ as well as of the MO anion itself. These calculated data showed, in the case of putative close anion–cation interactions, that the MO anions are partially sticking out of the dendrimers **5** and **7**, while the MO anions in **6** and **8** could be completely shielded by the aryl ether dendrons.

MALDI-TOF-MS was carried out for **5·4MO** to further confirm the proposed composition of the host–guest system. The MS-spectrum of **5·4MO** was complicated by the large number of ion peaks. Nevertheless, all the main peaks could be readily assigned, and characteristic peaks at m/z 2996.02 and 2692.85 were observed corresponding to the molecular and fragment ions $[\text{M}+\text{H}]^+$ (calcd for: 2996.19) and $[\text{M}-\text{MO}]^+$ (calcd for: 2691.84), respectively. The large number of other peaks is most probably due to in situ fragmentation processes (e.g., loss of multiple anions and the earlier mentioned C–N bond cleavage) and/or exchange with matrix anions. One of the main fragmentation patterns indicated the loss of an NMe_2 fragment that most likely originated from the complexed MO anions. For the larger composites (involving the dendrimers **6–8**), however, a clear confirmation of the proposed structures was more difficult due to an increased fragmentation behavior and matrix–MO anion exchange. Accordingly, no direct molecular ion was observed for **6·4MO**. However, illustrative in this respect is the presence of peaks at m/z 4239.3 (calcd for: 4239.4) and 4390.3 (calcd for: 4389.7), which were attributed to the fragment ions $[\text{M}+\text{DHB}-2\text{MO}]^+$ (DHB = 3,5-dihydroxy-benzoic acid) and $[\text{M}-\text{MO}]^+$, respectively. The latter indirectly pointed to the proposed host–guest stoichiometry. Under similar conditions, a fragment ion at m/z 5350.5 (calcd for: 5350.8) was observed for **7·8MO** (Figure 5A) which was ascribed to $[\text{M}-\text{MO}]^+$, while in the case of **8·8MO** a peak at m/z 8746.4 (assigned to $[\text{M}-\text{MO}]^+$) could be clearly detected (Figure 5B).

Mode of interaction between host and guest: To confirm that electrostatic interactions are the predominant attractive forces in these structures, we have studied the phase transfer of MO into CH_2Cl_2 by a sterically less congested model compound **10** (Scheme 4). This model compound was prepared analogously to **5–9** and isolated as a white solid in quantitative yield. Using the set-up depicted in Figure 4, this tetracationic derivative **10** was also found to form assemblies with MO anions. However, in contrast to the MO-assemblies of the core–shell dendrimeric species **5–9**, this particular MO-containing compound (i.e., **10·4MO**) is sparingly soluble

Scheme 4. Synthesis of the less congested dendritic species **10**.

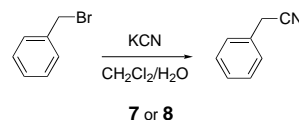
in aromatic solvents. This indicates a less efficient shielding of the ionic part by the Fréchet dendrons in this molecule.

^1H NMR spectroscopic quantification by specific signal integration (Table 2) suggested, just as in the case of **5** and **6**, the presence of four MO anions in **10**·**4MO**. This provided further evidence that the MO complexation by these cationic dendrimers is primarily based on electrostatic interactions. However, the possibility of π - π stacking between the aromatic parts in MO and the attached dendrons leading to an even larger stabilization of the host-guest system could not be excluded. To investigate this in more detail, compound **4** was also used as a potential phase-transfer agent. This derivative was also shown to be able to “extract” MO from the water layer and it seems therefore unlikely that π - π interactions play a pivotal role in the binding of MO anions by the cationic dendrimers **5**–**9**.

Scope of the new host-guest systems: In a subsequent study, several other inorganic/organic substrates were tested as possible guests for the dendritic hosts **5**–**8** by using similar procedures as described for the MO anion exchange procedure. The sodium salt of pyrene-1-sulfonic acid (Figure 4) was successfully extracted by the cationic dendrimer **5** from the water phase. The presence of anionic pyrene guests in **5** was evident from the recorded ^1H NMR spectrum, in which two distinctive doublets were found at $\delta = 9.41$ and 8.78 , which were attributed to H1 and H10 (see Figure 4). Also in this case, signal integration pointed to a full (i.e., four pyrene guests) loading in **5**. Interestingly, this material with anionic pyrene guest showed a much lower solubility in CH_2Cl_2 when compared to **5**·**4MO**.

Likewise, the formation of other guest molecule assemblies was also demonstrated by ^1H NMR spectroscopy. These other type of molecules include carboxylic acid derivatives such as methyl red (i.e., 4-(4-dimethylamino-phenylazo)benzoic acid), sulfates such as *p*-cresol sulfate, and chromate anions ($\text{Cr}_2\text{O}_7^{2-}$). The preliminary findings indicate that the polycationic dendrimer species **5**–**8** and **9** can bind different kinds of anionic inorganic/organic substrates.

Applications: We have investigated the potential use of the polycationic dendrimers **7** and **8** in phase-transfer catalysis. For this purpose, we selected the $\text{S}_{\text{N}}2$ reaction between (excess) potassium cyanide and benzyl bromide to afford benzyl cyanide (Scheme 5) under biphasic conditions (i.e., a $\text{CH}_2\text{Cl}_2/\text{H}_2\text{O}$ system). The formation of the nitrile product was

Scheme 5. $\text{S}_{\text{N}}2$ reaction between benzyl bromide and KCN catalyzed by **7** and **8** in a biphasic experiment.

monitored by ^1H NMR spectroscopy. Gradually a singlet resonance at $\delta = 3.75$ appeared while the singlet resonance corresponding to the CH_2Br group of the starting material decreased simultaneously. In the absence of **7** or **8** as a catalyst, minor formation of benzyl cyanide was observed after 20 h ($\leq 6\%$). However, in the presence of **7** and **8** (0.01 mol% catalytic ammonium groupings) a much higher conversion of 40 and 59%, respectively, was noted after 20 h. This clearly shows the suitability of these new polycationic dendrimers as micro-reactor systems.^[18]

Another interesting and rapid developing area in the field of dendrimer chemistry is the use of membrane technology. Membrane reactor systems in combination with catalytically active, nanosized metallodendrimers have recently been used to bridge the gap between homogeneous and heterogeneous catalysis.^[2d, e] These membrane experiments showed that recycling of dendrimer catalysts is very promising. We therefore anticipated that the newly presented host-guest systems, in which MO guests are bonded through electrostatic forces, would be retained by a suitable membrane filter.

To study this in more detail, a commercially available dialysis membrane with a cut-off mass of 1000 g mol^{-1} was loaded with the strongly orange-colored dendrimer **7**·**8MO** ($M_w = 5655 \text{ g mol}^{-1}$) and placed into a sealed system. After 72 h, no evidence for leaching of the dendrimer **7**·**8MO** into the bulk solution (CH_2Cl_2) could be obtained. Addition of an excess of $[\text{Bu}_4\text{N}]\text{PF}_6$ led to a fast colorization of the bulk CH_2Cl_2 solution ($< 1 \text{ h}$) and a slow, almost complete decolorization of the dialysis bag. The presence of the MO anion in the bulk solution could be confirmed by lowering the pH, which led to a fast color change from yellow/orange to purple/red. After repeated dialysis with $[\text{Bu}_4\text{N}]\text{PF}_6$ dissolved in CH_2Cl_2 , the contents of the dialysis membrane were subjected to NMR spectroscopic analysis (^1H , ^{19}F , and ^{31}P). The spectroscopic data were compared with the NMR spectroscopic data obtained for an authentic sample of **7**·**8PF}_6**. This comparison unambiguously revealed the presence of **7**·**8PF}_6** in the membrane vessel after this dialysis procedure and therefore indicated that dendrimer **7** already has an appropriate size for retention in a membrane system.

Conclusion

In summary, a synthetic strategy for the formation of stable assemblies based on a range of inorganic/organic substrates

and novel, cationic dendritic containers is presented. These polycationic dendrimers are quantitatively prepared with simple building blocks. The assembly of anionic, organic molecules with these cationic dendrimers is fully reversible and can be regulated by addition of other anions or lowering the pH of the medium. Moreover, the molecular containers can be fine-tuned with respect to the amount of potential guests by a predesign of the arylamine silane core or by changes in stoichiometry between host and guest. These characteristics make this type of molecular container extremely versatile for a range of applications. For example, these polycationic polymers have a great potential as dendritic microreactors while applications in controlled substrate delivery can be foreseen. In addition, the cavities in these dendrimers could be of great use in shape-selective (or phase-transfer) catalysis. Further studies are being carried out to explore the use of these polycationic dendrimers in a number of these applications as well as a more detailed investigation of the location of the anionic guest molecules in these polycationic dendrimers.

Experimental Section

General: All air-sensitive manipulations were carried out in an inert atmosphere using standard Schlenk techniques. All solvents were carefully dried and distilled prior to use. Standard chemicals were purchased from Acros Chimica or Aldrich and used without further purification. The compounds **1b**,^[7] [G1]-Br,^[12a] and [G2]-Br^[12a] were prepared according to previously reported procedures. ¹H, ¹³C{¹H}, ³¹P, ¹⁹F, and ²⁹Si{¹H} NMR spectroscopic measurements were carried out on a Varian Inova/Mercury 200 or 300 MHz spectrometer at 25 °C and chemical shifts (δ) are given in ppm with TMS or H₃PO₄ as external standards or relatively to the residual solvent peak. The MALDI-TOF mass spectra were acquired using a Voyager-DE BioSpectrometry Workstation mass spectrometer (PerSeptive Biosystems Inc., Framingham, MA, USA). ES-MS spectra were obtained from the Analytical Chemistry department, Utrecht University. Elemental analyses were performed by Dornis und Kolbe, Mülheim/Ruhr, Germany.

Si(CN)₄ (1b): tBuLi (15 mL, 1.5 M in pentane, 22.5 mmol) was added at –78 °C to a solution of 1-bromo-4-[(dimethylamino)methyl]-benzene (2.79 g, 13.0 mmol) dissolved in THF (40 mL). The resulting white suspension was stirred for about 10 min and subsequently SiCl₄ (0.3 mL, 2.6 mmol) was added. After the mixture reached RT, the suspension was stirred for an additional period of 19 h. The reaction mixture was quenched with an excess of H₂O. The organic layer was separated and the H₂O layer extracted with pentane (2 × 40 mL). The solvent was removed under reduced pressure to give a yellow viscous oil. To remove siloxane impurities, the yellow oily product was filtered through a path of silica with CH₂Cl₂/NEt₃ 120:1 v/v as eluent and recrystallized from pentane to afford **1b** as a white solid material (0.70 g, 1.24 mmol, 47%). ¹H NMR (200 MHz, C₆D₆): δ = 7.80 (d, 8H, ³J = 7.6 Hz, ArH), 7.38 (d, 8H, ³J = 7.6 Hz, ArH), 3.26 (s, 8H, CH₂N), 2.07 (s, 24H, N(CH₃)₂); ¹³C{¹H} NMR (50 MHz, C₆D₆): δ = 141.5, 137.0, 133.6, 128.3 (ArC), 64.5 (CH₂N), 46.6 (N(CH₃)₂); MS (MALDI-TOF, DHB): *m/z*: 565.8 [M+H]⁺; elemental analysis calcd (%) for C₃₆H₄₈N₄Si (565.9): C 76.54, H 8.57, N 9.92, Si 4.67; found: C 76.39, H 8.67, N 9.85, Si 4.85.

Preparation of model compounds: *General procedure:* The polycationic compounds **2–4** were prepared by mixing **1a** with an excess of MeI, EtBr, or octyl iodide in CH₂Cl₂ and the initially clear reaction mixtures were stirred at room temperature (<24 h). After removal of all volatiles, the products were obtained as white solids by washing with pentane and drying in vacuo.

Si(CN)₄·8MeI (2): White solid (0.41 g, 85%); m.p. 73–74 °C; ¹H NMR (200 MHz, D₂O): δ = 8.19 (s, 8H, ArH), 7.88 (s, 4H, ArH), 4.62 (s, 16H, CH₂N), 3.16 (s, 72H, N(CH₃)₂); ¹³C{¹H} NMR (75 MHz, D₂O): δ = 145.3, 142.4, 137.9, 131.8 (4 × ArC), 71.0 (CH₂N), 55.7 (N(CH₃)₂); MS (FAB): *m/z*:

1801 [M–I]⁺; elemental analysis calcd (%) for C₅₆H₁₀₀N₈Si₈ (1928.8): C 34.87, H 5.23, N 5.81, Si 1.46; found: C 34.89, H 5.26, N 5.74, Si 1.57.

Si(CN)₄·8EtBr (3): White solid (170 mg, >99%); m.p. 76–77 °C; ¹H NMR (200 MHz, D₂O): δ = 8.04 (s, 8H, ArH), 7.88 (s, 4H, ArH), 4.61 (s, 16H, ArCH₂N), 3.41 (q, 16H, *J* = 7.0 Hz, CH₂CH₃), 3.03 (s, 48H, N(CH₃)₂), 1.36 (t, 24H, *J* = 7.0 Hz, CH₂CH₃); ¹³C{¹H} NMR (50 MHz, D₂O): δ = 142.6, 139.5, 134.6, 128.7 (4 × ArC), 66.0 (Ar–CH₂N), 60.2 (CH₂), 49.1 (N(CH₃)₂), 7.8 (CH₃); MS (FAB): *m/z*: 1585.1 [M–Br]⁺; elemental analysis calcd (%) for C₆₄H₁₁₆N₈Si₈Br₈ (1665.0): C 46.17, H 7.02, N 6.73, Si 1.69; found: C 46.28, H 7.08, N 6.73, Si 1.75.

Si(CN)₄·8octyl-I (4): Off-white solid (0.20 g, 73%); m.p. 75–76 °C; ¹H NMR (200 MHz, CDCl₃): δ = 8.36 (m, 4H, ArH), 8.32 (m, 8H, ArH), 5.11 (brs, 16H, ArCH₂N), 3.65 (m, 16H, CH₂CH₂N), 3.26 (brs, 48H, N(CH₃)₂), 1.79 (m, 16H, CH₂CH₂N), 1.66 (m, 32H, –CH₂–, octyl), 1.35–1.25 (m, 48H, –CH₂–, octyl), 0.88 (t, 24H, CH₃, octyl); ¹³C{¹H} NMR (50 MHz, CDCl₃): δ = 142.9, 140.8, 135.6, 128.9 (4 × ArC), 66.4 (ArCH₂N), 65.3 (CH₂CH₂N), 49.8 (N(CH₃)₂), 31.7, 29.2, 29.1, 26.3, 22.9, 22.6 (6 × CH₂, octyl), 14.1 (CH₃, octyl); MS (FAB): *m/z*: 2587.0 [M+H–I]⁺; elemental analysis calcd (%) for C₁₁₂H₂₁₂N₈Si₈ (2714.3): C 49.56, H 8.87, N 4.13; found: C 49.83, H 7.78, N 4.87.

Si(CN)₄·4[G1]-Br (5): A mixture of **1b** (0.18 g, 0.31 mmol) and [G1]-Br (0.48 g, 1.25 mmol) in CH₂Cl₂ (25 mL) was stirred for 3 d at room temperature under nitrogen. The slightly yellow reaction mixture was then filtered through a path of Celite, dried over MgSO₄, and concentrated in vacuo. The product was isolated in quantitative yield as a white solid. ¹H NMR (300 MHz, CDCl₃): δ = 7.77 (brd, 8H, ³J = 8.4 Hz, ArH), 7.40–7.10 (m, 48H, ArH), 6.73 (brs, 8H, ArH), 6.71 (brs, 4H, ArH), 5.37 (brs, 8H, CH₂N), 5.05 (brs, 8H, OCH₂), 4.80 (brs, 8H, NCH₂), 2.98 (brs, 24H, NMe₂); ¹³C{¹H} NMR (75 MHz, CDCl₃): δ = 160.1, 136.8, 136.3, 135.1, 133.4, 130.0, 128.9, 128.7, 127.9, 112.6, 104.1 (ArC), 70.4 (broad, overlapping CH₂N), 67.5 (CH₂O), 48.8 (N(CH₃)₂); MS (ES, THF): *m/z*: 969.3 [M–2Br]²⁺, 777.7 [M–[G1]-Br–2Br]²⁺, 619.7 [M–3Br]³⁺, 492.0 [M–[G1]-Br–3Br]³⁺, 444.9 [M–4Br]⁴⁺; elemental analysis calcd (%) for C₁₂₀H₁₂₄Br₄N₄O₈Si₈·8H₂O (2242.1): C 64.28, H 6.29, N 2.50; found: C 64.25, H 6.08, N 2.51.

Si(CN)₄·4[G2]-Br (6): A mixture of **1b** (79.3 mg, 0.14 mmol) and [G2]-Br (0.44 g, 0.54 mmol) in freshly distilled CH₂Cl₂ (25 mL) was stirred for 24 h at room temperature under nitrogen. The slightly yellow reaction mixture was concentrated in vacuo, and the residue was washed with Et₂O (5 × 50 mL). The product was isolated as a white pellet by centrifugation, dissolved in CH₂Cl₂, dried over MgSO₄, filtered, and concentrated in vacuo to give **6** as a white solid in quantitative yield. ¹H NMR (300 MHz, CDCl₃): δ = 7.76 (m, 8H, ArH), 7.60–6.90 (brm, 96H, ArH), 6.73, 6.65, 6.62, 6.49 (brm, 36H, ArH), 5.10–4.60 (br signal, 64H, all CH₂ groups), 2.97 (brs, 24H, N(CH₃)₂); ¹³C{¹H} NMR (75 MHz, CDCl₃): δ = 160.1, 138.7, 136.7, 133.3, 129.9, 128.8, 128.5, 128.0, 127.6, 112.3, 106.6, 104.0, 101.6 (ArC), 70.0 (br, overlapping CH₂N), 67.5 (br, overlapping CH₂O), 48.7 (br, N(CH₃)₂); MS (ES, THF): *m/z*: 1818.6 [M–2Br]²⁺, 1413.9 [M–[G2]-Br–Br]²⁺, 1185.5 [M–3Br]³⁺, 916.2 [M–[G2]-Br–2Br]²⁺, 869.3 [M–4Br]⁴⁺; elemental analysis calcd (%) for C₂₃₂H₂₂₀Br₄N₄O₂₄Si₈ (3796.0): C 73.41, H 5.84, N 1.48, Br 8.42; found: C 73.62, H 5.91, N 1.54, Br 8.34.

Si(CN)₄·8[G1]-Br (7): A mixture of **1a** (0.10 g, 0.13 mmol) and [G1]-Br (0.45 g, 1.40 mmol) in freshly distilled CH₂Cl₂ (25 mL) was stirred for 96 h at room temperature under nitrogen. The slightly yellow reaction mixture was concentrated in vacuo, whereupon Et₂O (15 mL) was added to the residue. The resultant mixture was stirred for 24 h, and the crude product was isolated by centrifugation. The product was washed with Et₂O (15 mL) to remove the excess of [G1]-Br and isolated in quantitative yield after drying in vacuo. ¹H NMR (300 MHz, CDCl₃): δ = 8.41 (brs, 8H, ArH), 8.19 (brs, 4H, ArH), 7.29–7.15 (m, 80H, ArH), 7.00 (brs, 16H, ArH), 6.57 (brs, 8H, ArH), 5.19 (brs, 48H, OCH₂+CH₂N), 4.84 (brs, 16H, NCH₂), 3.07 (brs, 48H, NMe₂); ¹³C{¹H} NMR (75 MHz, CDCl₃): δ = 159.8, 143.3, 140.5, 136.3, 135.4, 129.3, 128.6, 128.4, 128.0, 127.7, 112.5, 104.2 (ArC), 70.2 (OCH₂), 67.7, 66.0 (CH₂NCH₂), 48.8 (N(CH₃)₂); MS (ES, THF): *m/z*: 1849.8 [M–2Br]²⁺, 1206.5 [M–3Br]³⁺, 1078.8 [M–[G1]-Br–3Br]³⁺, 884.8 [M–4Br]⁴⁺, 789.1 [M–[G1]-Br–4Br]⁴⁺, 597.6 [M–3[G1]-Br–4Br]⁴⁺; elemental analysis calcd (%) for C₂₁₆H₂₂₈N₈Br₈O₁₆Si₈ (3859.5): C 67.22, H 5.95, N 2.90, Br 16.56; found: C 67.38, H 5.86, N 2.82, Br 16.68.

Si(CN)₄·8[G2]-Br (8): A mixture of **1a** (58 mg, 73 mol) and [G2]-Br (0.48 g, 0.59 mmol) in freshly distilled CH₂Cl₂ (25 mL) was stirred for 24 h

at room temperature under nitrogen. The slightly yellow reaction mixture was concentrated in vacuo, and the residue was washed with Et₂O (5 × 50 mL). The product was isolated as a white solid by centrifugation, dissolved in CH₂Cl₂, dried over MgSO₄, filtered, and concentrated in vacuo to give **8** in quantitative yield. ¹H NMR (300 MHz, CDCl₃): δ = 8.35 (brs, 8H, ArH), 7.89 (brs, 4H, ArH), 7.27–6.98 (brm, 160H, ArH), 6.58, 6.54, 6.41 (br overlapping signals, 72H, ArH), 4.95–4.50 (m, 128H, all CH₂ groups), 3.00 (brs, 48H, N(CH₃)₂); ¹³C{¹H} NMR (75 MHz, CDCl₃): δ = 160.1, 159.9, 139.0, 136.8, 129.4, 128.6, 128.0, 127.8, 112.5, 106.7, 104.5, 101.6 (ArC), 70.0 (br, all CH₂O), 67.6 (br, all CH₂N), 48.9 (br, N(CH₃)₂); MS (ES, THF): *m/z*: 2338.7 [M–3Br]³⁺; elemental analysis calcd (%) for C₄₄₀H₄₂₀N₈Br₈O₄₈Si (7255.5): C 72.84, H 5.83, N 1.54; found: C 72.68, H 5.96, N 1.53.

[G1]-SiMe₂-NCN·24[G1]-Br (9): A mixture of [G1]-SiMe₂-NCN (0.19 g, 0.0499 mmol) and [G1]-Br (0.45 g, 1.17 mmol) in CH₂Cl₂ (30 mL) was stirred for 20 h. Subsequently the solvent was removed in vacuo and the remaining solid washed with Et₂O (50 mL) to yield **9** as an off-white solid (0.64 g, 0.0492 mmol, 99%). ¹H NMR (200 MHz, CDCl₃): δ = 8.14 (m, 36H, ArH), 7.26 (brm, ArH), 6.90 (s, 48H, ArH), 6.60 (s, 24H, ArH), 5.14 (brs, 48H, CH₂N), 5.00 (brs, 96H, CH₂O), 4.50 (brs, 48H, NCH₂), 3.06 (brs, 144H, N(CH₃)₂), 1.20, 0.84, 0.49 (3 × m, 96H, SiCH₂CH₂CH₂Si), 0.26 (brs, 72H, Si(CH₃)₂); ¹³C{¹H} NMR (75 MHz, CDCl₃): δ = 159.95, 149.87, 143.17, 140.90, 137.78, 136.22, 129.17, 128.52, 128.05, 127.73, 112.43, 104.05 (12 × ArC), 70.21 (CH₂O), 67.65, 66.99 (2 × CH₂N), 48.86 (N(CH₃)₂), 20.27, 18.65, 17.41 (SiCH₂CH₂CH₂Si, overlapping signals), –2.55 (Si(CH₃)₂); ²⁹Si{¹H} NMR (60 MHz, CDCl₃): δ = 0.77 (br signal, Si_{core}+Si_{inner}), –2.07 (br, SiMe₂Ph); MS (ES, CH₃CN): *m/z*: 3171.4 [M–4Br]⁴⁺, 3075.9 [M–[G1]-Br–4Br]⁴⁺, 2521.5 [M–5Br]⁵⁺, 2444.9 [M–[G1]-Br–5Br]⁵⁺, 2088.0 [M–6Br]⁶⁺, 2023.93 [M–[G1]-Br–6Br]⁶⁺; elemental analysis calcd (%) for C₇₂₀H₈₅₂N₂₄Si₁₇O₄₈Br₂₄ (13006): C 66.49, H 6.60, N 2.58, Br 14.75; found: C 67.06, H 6.39, N 2.44, Br 14.28.

Me₂Si(NCN)₂·4[G1]-Br (10): This compound was prepared in a similar way as described for **5–8**. A mixture of Me₂Si(NCN)₂^[19] (0.21 g, 0.48 mmol) and [G1]-Br (0.70 g, 1.97 mmol) in CH₂Cl₂ (25 mL) was stirred for 4 h. The solvent was removed under reduced pressure and the solid residue was washed with Et₂O to give **10** as a white solid (0.75 g, 0.40 mmol, 84%). ¹H NMR (200 MHz, CDCl₃): δ = 8.35 (s, 2H, ArH), 8.20 (s, 4H, ArH), 7.34–7.24 (m, 40H, ArH), 6.91 (s, 6H, ArH), 6.64 (s, 3H, ArH), 5.00 (s, 16H, CH₂O), 4.77 (s, 16H, overlapping CH₂N), 3.02 (s, 24H, N(CH₃)₂), 0.63 (s, 6H, Si(CH₃)₂); ¹³C{¹H} NMR (50 MHz, CDCl₃): δ = 160.2, 141.8, 141.0, 136.5, 129.2, 128.9, 128.6, 128.4, 128.2, 127.8, 112.8, 104.7 (ArC), 70.5 (CH₂O), 67.6 (br, overlapping CH₂N), 49.2 (br, NCH₂), –2.0 (br, Si(CH₃)₂); elemental analysis calcd (%) for C₁₀₂H₁₂₀N₄SiO₈Br₄ (1973.9): C 65.24, H 6.44, N 2.98; found: C 65.38, H 6.38, N 2.90.

Preparation and characterization of MO-dendrimer assemblies: All solutions were prepared at room temperature in the presence of air, using freshly distilled CH₂Cl₂ and de-ionized water. Two stock solutions were prepared: A solution of one of the dendrimer species in dichloromethane (3 × 10^{–4}–8 × 10^{–4} M) and a solution of methyl orange in water. In a typical procedure, five two-phase systems were prepared in such manner that the ratio between bromide anions in the dendrimer and methyl orange anions ranged from 1:4 to 5:4 (in the case of **5** and **6**) or from 2:8 to 10:8 (in the case of **7** and **8**). The two-phase systems were mixed for 20 h and then the layers were separated for analysis. The water layers were diluted to such an extent that the ultimate amount of methyl orange still present in the water layers could be determined with UV/Vis absorption spectroscopy using a calibration curve derived from a series of samples with known concentrations of methyl orange in water. The UV/Vis experiments evidenced that the dendrimer systems are only able to exchange either a maximum of 4 or 8 MO anions, whereas an excess of MO remains in the H₂O layer of the two-phase system. The dichloromethane layers were washed with water, dried over Na₂SO₄, and concentrated in vacuo. The isolated orange solids were analyzed with ¹H NMR spectroscopy in CDCl₃ and with MALDI-TOF-MS. The peak assignments were based on the appearance of new signals in the ¹H NMR spectra, which were attributed to the presence of MO anions and on a stepwise increase in Δδ for several groups of the dendrimers upon assembly with an increasing number of MO anions. From the obtained data, the maximum amount of MO in the (dendrimeric) assemblies (i.e., **5–10**) was calculated and these results are summarized in Table 2 (see main text).

For **5·4MO** (*M_w* = 2995.8): ¹H NMR (300 MHz, CDCl₃): δ = 8.02 (d, *J* = 8.1 Hz, 8H, ArH(MO)), 7.78 (d, *J* = 9.0 Hz, 8H, ArH(MO)), 7.69 (d, *J* = 7.8 Hz, 8H, ArH(MO)), 7.26–7.18 (m, 56H, ArH), 6.68 (d, *J* = 9.3 Hz, 8H, ArH(MO)), 5.20 (brs, 8H, ArCH₂), 4.90 (s, 16H, ArOCH₂), 4.63 (brs, 8H, ArCH₂), 3.02 (s, 24H, NMe₂(MO)), 2.83 (brs, 24H, core NMe₂); MS (MALDI-TOF, DHB): *m/z*: 3298.8 [M+2DHB]⁺, 3147.8 [M+DHB]⁺, 2996.0 [M+H]⁺, 2800.2 [M–MO–NMe₂+DHB]⁺, 2692.9 [M–MO]⁺, 2648.7 [M–MO–NMe₂]⁺, 2496.6 [M–2MO–NMe₂+DHB]⁺, 2345.7 [M–2MO–NMe₂]⁺, 2194.6 [M–3MO–NMe₂+DHB]⁺, 2150.6 [M–3MO–2NMe₂+DHB]⁺.

Dendrimer **6·4MO** (*M_w* = 4693.8): ¹H NMR (300 MHz, CDCl₃, 60 °C): δ = 8.02 (brd, *J* = 8.1 Hz, 8H, ArH(MO)), 7.71 (brd, *J* = 9.0 Hz, 8H, ArH(MO)), 7.65 (brd, *J* = 8.7 Hz, 8H, ArH(MO)), 7.31–7.19 (m, 96H, ArH), 6.71 (brs, 8H, ArH), 6.61–6.58 (br, 24H, overlapping ArH(MO), ArH), 6.46 (brs, 12H, ArH), 4.90, 4.83, 4.66 (brs, 64H, all ArOCH₂, ArCH₂), 2.95 (s, 24H, NMe₂(MO)), 2.88 (brs, 24H, core NMe₂); MS (MALDI-TOF, DHB): *m/z*: 4239.3 [M+DHB–2MO]⁺, 4390.3 [M–MO]⁺

Dendrimer **7·8MO** (*M_w* = 5655.1): ¹H NMR (200 MHz, CDCl₃): δ = 8.88 (brs, 8H, ArH_{core}), 8.75 (brs, 4H, ArH_{core}), 7.89 (d, *J* = 8.4 Hz, 16H, ArH(MO)), 7.79 (d, *J* = 8.8 Hz, 16H, ArH(MO)), 7.69 (d, *J* = 8.6 Hz, 16H, ArH(MO)), 7.18 (m, 80H, ArH), 6.69 (d, *J* = 9.2 Hz, 16H, ArH(MO)), 6.67 (brs, 16H, ArH), 6.52 (brs, 8H, ArH), 4.80 (m, 48H, overlapping ArCH₂ and ArOCH₂), 4.54 (brs, 16H, ArCH₂), 3.04 (s, 48H, NMe₂(MO)), 2.78 (brs, 48H, core NMe₂); MS (MALDI-TOF, DHB): *m/z*: 5350.5 [M–MO]⁺.

Dendrimer **8·8MO** (*M_w* = 9051.1): ¹H NMR (200 MHz, CDCl₃): δ = 8.92 (brs, 8H, ArH_{core}), 8.72 (brs, 4H, ArH_{core}), 7.87 (brd, *J* not resolved, 16H, ArH(MO)), 7.71 (brd, *J* = 8.1 Hz, 16H, ArH(MO)), 7.66 (brd, *J* not resolved, 16H, ArH(MO)), 7.23 (brm, 160H, ArH), 6.76, 6.47, 6.38 (m, 88H, ArH+ArH(MO)), 4.76, 4.70 (m, 128H, all ArOCH₂+ArCH₂), 2.93 (brs, 48H, NMe₂(MO)), 2.81 (brs, 48H, core NMe₂); MS (MALDI-TOF, DHB): *m/z*: 8746.4 [M–MO]⁺, 8443.1 [M–2MO+H]⁺.

Dendrimer **9·24MO** (*M_w* = 18393): ¹H NMR (200 MHz, CDCl₃): δ = 8.10 (m, 84H, ArH_{core}), 7.92 (brd, *J* = 6.8 Hz, 48H, ArH(MO)), 7.73 (brd, *J* = 8.8 Hz, 48H, ArH(MO)), 7.65 (brd, *J* = 8.2 Hz, 48H, ArH(MO)), 7.18 (m, 240H, ArH), 6.72 (brs, 48H, ArH), 6.59 (brd, *J* = 8.4 Hz, 48H, ArH(MO)), 6.49 (brs, 24H, ArH), 4.81 (m, 192H, all ArOCH₂+ArCH₂), 2.95 (s, 144H, NMe₂(MO)), 2.85 (brs, 144H, core NMe₂), 1.25 (brm, SiCH₂CH₂CH₂Si), 0.88 (brm, SiCH₂CH₂CH₂Si), 0.68 (brm, SiCH₂CH₂CH₂Si), 0.26 (brs, 72H, carbosilane dendrimer CH₂); MS (MALDI-TOF, DHB): *m/z*: ≈ 10000–15000 (broad peak).

Dendrimer **10·4MO** (*M_w* = 2871.7): ¹H NMR (200 MHz, CDCl₃): δ = 8.55 (s, 2H, ArH_{core}), 8.37 (s, 4H, ArH_{core}), 7.98 (d, 8H, *J* = 9.2 Hz, ArH(MO)), 7.85 (d, 8H, *J* = 8.6 Hz, ArH(MO)), 7.76 (d, 8H, *J* = 8.0 Hz, ArH(MO)), 7.32–7.25 (m, 40H, ArH), 6.75–6.63 (m, 20H, ArH+ArH(MO)), 6.64 (s, 3H, ArH), 4.95 (m, 24H, CH₂O+CH₂N), 4.53 (s, 8H, CH₂N), 3.09 (s, 24H, NMe₂(MO)), 2.92 (brs, 24H, core NMe₂), 0.08 (s, 6H, Si(CH₃)₂); ¹³C{¹H} NMR (50 MHz, CDCl₃): δ = 160.19, 152.79, 147.13, 143.60, 141.26, 139.44, 136.46, 129.01, 128.71, 128.17, 127.90, 126.88, 125.57, 122.20, 112.29, 111.77, 104.75 (17 ArC), 70.37 (CH₂O), 68.50 (br, overlapping CH₂N), 49.08 (br, NCH₂), 40.61 (N(CH₃)₂, MO), –3.23 (br, Si(CH₃)₂); MS (MALDI-TOF, DHB): *m/z*: 2566.1 [M–MO]⁺, 1958.7 [M–3MO]⁺.

Phase-transfer catalysis: A typical experiment is as follows: A mixture of KCN (0.28 g, 430 μmol) in H₂O (5 mL), benzyl bromide (0.19 g, 111 μmol) in CH₂Cl₂ (5 mL) and **8** (10.6 mg, 0.012 mmol catalytic ammonium groups) was stirred vigorously at ambient temperature. Samples for ¹H NMR spectroscopic analysis were taken after 3 and 20 h. Conversions were determined by signal integration and compared with the noncatalyzed run.

Membrane experiment: A commercially available dialysis membrane with a cut-off mass of 1000 g mol^{–1} (SIGMA) was loaded with a solution of **7·8MO** (7.0 mg, 1.24 μmol) in CH₂Cl₂ (ca. 10 mL). The contents of the dialysis tubing were placed into a sealed system containing CH₂Cl₂ (300 mL) and H₂O (0.5 mL). After 3 d of gently stirring and replacing the CH₂Cl₂/H₂O mixture twice, an excess of NBu₄PF₆ (4.8 g) was added to the bulk solution. The dialysis tubing slowly started to decolorize with a simultaneous colorization of the CH₂Cl₂ bulk solution. The bulk solution was replaced two times within 3 d with a dialysis solution of NBu₄PF₆ (4.2–4.5 g) in CH₂Cl₂. Then the dialysis bag was thoroughly washed with CH₂Cl₂ to remove excess of NBu₄PF₆ still present in the tubing and subsequently

disconnected from the set-up. After isolation of the contents by extraction with CH_2Cl_2 and drying in vacuo, an off-white solid was obtained which was subjected to NMR spectroscopic analysis. The whole procedure was carried out twice and confirmed the reproducibility of the membrane experiment. The NMR spectroscopic data was compared with an authentic sample of **7·8PF₆**, which was synthesized by a similar procedure as described for the MO-containing dendrimers using the two-phase system depicted in Figure 4 loaded with **7** (in CH_2Cl_2) and an excess of sodium hexafluorophosphate (in H_2O). Spectroscopic data for **7·8PF₆**: ^1H NMR (300 MHz, CDCl_3): $\delta = 8.01$ (brs, 8H, ArH), 7.86 (s, 4H, ArH), 7.33–7.25 (brm, 40H, ArH), 6.68 (s, 8H, ArH), 6.47 (brs, 16H, ArH), 5.01 (brs, 32H, CH_2O), 4.06 (brs, 16H, CH_2NCH_2), 3.77 (brs, 16H, CH_2NCH_2), 2.62–2.47 (brs, 48H, $\text{N}(\text{CH}_3)_2$); ^{19}F NMR (282 MHz, CDCl_3): $\delta = -70.30$ (d, $^1J(\text{F,P}) = 714$ Hz); ^{31}P NMR (81 MHz, CDCl_3): $\delta = -143.14$ (m, $^1J(\text{F,P}) = 714$ Hz).

Crystal data and data collection

Crystal data for 3: $\text{C}_{56}\text{H}_{100}\text{N}_8\text{Si}_8$ +solvent; colorless block-shaped crystal ($0.40 \times 0.25 \times 0.20$ mm), $M_w = 1928.8$ (excluding solvent), triclinic, space group $P\bar{1}$ (no. 2), with $a = 13.803(4)$, $b = 15.634(2)$, $c = 22.290(6)$ Å, $\alpha = 98.89(2)^\circ$, $\beta = 93.89(2)^\circ$, $\gamma = 103.16(2)^\circ$, $V = 4600.7(19)$ Å³, $Z = 2$, $\rho_{\text{calcd}} \approx 1.51$ g cm⁻³, $\mu(\text{MoK}\alpha) = 2.6$ mm⁻¹. X-ray data were collected on a Nonius CAD4T diffractometer (rotating anode, $\text{MoK}\alpha$ radiation, $T = 150$ K, ω scan, $\theta_{\text{max}} = 27.5^\circ$). Data were corrected for absorption using psi-scan data. The structure was solved by Direct Methods (SHELXS97) and refined on F^2 (SHELXL97). The cation could be refined with anisotropic thermal parameters for the non-hydrogen atoms. Hydrogen atoms were taken into account at calculated positions. Several of the iodine anions were found to be disordered over several sites. In addition, the crystal structure contains several solvent molecules of crystallisation. Due to their positional disorder their nature could not be identified satisfactorily. A disorder model with partially occupied sites was refined to take the scattering matter into account in the structure factor calculations. Convergence was reached at $R = 0.11$ for 7799 reflections with $I > 2\sigma(I)$ and 730 parameters ($wR2 = 0.36$). A residual density map showed no features apart from absorption artifacts near iodine.

Crystallographic data (excluding structure factors) for the structure of **2** reported in this paper have been deposited with the Cambridge Crystallographic Data Centre as supplementary publication no. CCDC-102002. Copies of the data can be obtained free of charge on application to CCDC, 12 Union Road, Cambridge CB21EZ, UK (fax: (+44)1223-336-033; e-mail: deposit@ccdc.cam.ac.uk).

Acknowledgement

A.W.K. and A.L.S. thank the Council for Chemical Sciences (CW) from the Dutch Organization for Scientific Research (NWO) for financial support. Cees Versluis from the Department of Analytical Chemistry of the University of Utrecht is gratefully acknowledged for the electrospray mass spectrometric studies. We thank Prof. Dr. Ashok Kakkar for stimulating suggestions during the preparation of this manuscript.

- [1] For recent reviews on dendritic molecules see: a) M. A. Hearshaw, J. R. Moss, *Chem. Commun.* **1999**, 1–8; b) A. W. Bosman, H. M. Janssen, E. W. Meijer, *Chem. Rev.* **1999**, 99, 1665–1688; c) G. Newkome, E. He, C. N. Moorefield, *Chem. Rev.* **1999**, 99, 1689–1746; d) J. P. Majoral, A. M. Caminade, *Chem. Rev.* **1999**, 99, 845–880; e) M. Fischer, F. Vögtle, *Angew. Chem.* **1999**, 111, 934–955; *Angew. Chem. Int. Ed.* **1999**, 38, 884–905; f) J. M. J. Fréchet, C. J. Hawker, I. Gitsov, J. W. Leon, *J. Macromol. Sci. Pure Appl. Chem.* **1996**, A33, 1399–1425; g) D. A. Tomalia, H. D. Durst, *Top. Curr. Chem.* **1993**, 165, 193–313.
- [2] For examples of dendrimers with catalytic end groups see: a) J. W. J. Knapen, A. W. van der Made, J. C. De Wilde, P. W. M. N. van Leeuwen, P. Wijkens, D. M. Grove, G. van Koten, *Nature* **1994**, 372, 659–663; b) M. T. Reetz, G. Lohmer, R. Schwikardi, *Angew. Chem.* **1997**, 109, 1559–1562; *Angew. Chem. Int. Ed. Engl.* **1997**, 36, 1526–1529; c) A. W. Kleij, R. A. Gossage, J. T. B. H. Jastrzebski, J. Boersma, G. van Koten, *Angew. Chem.* **2000**, 112, 182–185; *Angew. Chem. Int. Ed.* **2000**, 39, 179–181. Recently, the use of these catalytic materials in membrane reactors to facilitate catalyst recovery has been demonstrated. See: d) N. J. Hovestad, E. B. Eggeling, H. J. Heidebüchel, J. T. B. H. Jastrzebski, U. Kragl, W. Keim, D. Vogt, G. van Koten, *Angew. Chem.* **1999**, 111, 1763–1765; *Angew. Chem. Int. Ed.* **1999**, 38, 1655–1658; e) N. Brinkmann, D. Giebel, G. Lohmer, M. T. Reetz, U. Kragl, *J. Catal.* **1999**, 183, 163–168.
- [3] For relevant examples of dendrimers acting as (inverted) micelles and/or molecular containers, see: a) G. Caminati, N. J. Turro, D. A. Tomalia, *J. Am. Chem. Soc.* **1990**, 112, 8515–8522; b) K. R. Gopidas, A. R. Leheny, G. Caminati, N. J. Turro, D. A. Tomalia, *J. Am. Chem. Soc.* **1991**, 113, 7335–7342; c) G. Newkome, C. N. Moorefield, G. R. Baker, M. J. Saunders, S. H. Grossman, *Angew. Chem.* **1991**, 103, 1207–1209; *Angew. Chem. Int. Ed. Engl.* **1991**, 30, 1178–1180; d) C. J. Hawker, K. L. Wooley, J. M. J. Fréchet, *J. Chem. Soc. Perkin Trans. 1* **1993**, 1287–1297; e) J. F. G. A. Jansen, E. M. M. de Brabander-van den Berg, E. W. Meijer, *Science* **1994**, 266, 1226–1229; f) J. F. G. A. Jansen, E. M. M. de Brabander-van den Berg, E. W. Meijer, *J. Am. Chem. Soc.* **1995**, 117, 4417–4418; g) S. Stevelmans, J. C. M. van Hest, J. F. G. A. Jansen, D. A. F. J. van Bostel, E. M. M. de Brabander-van den Berg, E. W. Meijer, *J. Am. Chem. Soc.* **1996**, 118, 7398–7399; h) A. I. Cooper, J. D. Londono, G. Wignall, J. B. McClain, E. T. Samulski, J. S. Lin, A. Dobrynin, M. Rubinstein, A. L. C. Burke, J. M. J. Fréchet, J. M. DeSimone, *Nature* **1997**, 389, 368–371; i) M. W. P. L. Baars, P. E. Froehling, E. W. Meijer, *Chem. Commun.* **1997**, 1959–1960; j) V. Chechik, M. Zhao, R. M. Crooks, *J. Am. Chem. Soc.* **1999**, 121, 4910–4911; k) C. Loup, M. A. Zanta, A. M. Caminade, J. P. Majoral, B. Meunier, *Chem. Eur. J.* **1999**, 5, 3644–3650; l) H. Stephan, H. Spies, B. Johannsen, L. Klein, F. Vögtle, *Chem. Commun.* **1999**, 1875–1876.
- [4] G. Pistolis, A. Malliaris, D. Tsiourvas, C. Paleos, *Chem. Eur. J.* **1999**, 5, 1440–1444.
- [5] For examples see: a) G. R. Newkome, B. D. Woosley, E. He, C. N. Moorefield, R. Güther, G. R. Baker, G. H. Escamilla, J. Merrill, H. Luftmann, *Chem. Commun.* **1996**, 2737–2738; b) G. R. Newkome, C. N. Moorefield, G. R. Baker, US Pat. 5650101, **1999**; [*Chem. Abstr.* **1999**, 69896]; c) G. R. Newkome, Z. Yao, G. R. Baker, V. K. Gupta, *J. Org. Chem.* **1985**, 50, 2003–2004. For a relevant example of polycationic dendrimers see: d) C. Larr, B. Donnadieu, A. M. Caminade, J. P. Majoral, *J. Am. Chem. Soc.* **1998**, 120, 4029–4030.
- [6] For a review on host–guest complexation including electrostatic forces see: H. J. Schneider, *Angew. Chem.* **1991**, 103, 1419–1439; *Angew. Chem. Int. Ed. Engl.* **1991**, 30, 1417–1436.
- [7] A. W. Kleij, H. Klein, J. T. B. H. Jastrzebski, W. J. J. Smeets, A. L. Spek, G. van Koten, *Organometallics* **1999**, 18, 268–276.
- [8] P. R. Ashton, K. Shibata, A. N. Shipway, J. F. Stoddart, *Angew. Chem.* **1997**, 109, 2902–2904; *Angew. Chem. Int. Ed. Engl.* **1997**, 36, 2781–2783.
- [9] a) Z. Wu, K. Biemann, *Int. J. Mass Spectrom. Ion Processes* **1997**, 165/166, 349–361. For the synthesis of the studied dendritic cations/anions see: b) S. W. Kraska, D. Seyferth, *J. Am. Chem. Soc.* **1998**, 120, 3604–3612.
- [10] See for instance: J. March, *Advanced Organic Chemistry*, 4th ed., Wiley, New York, **1992**, pp. 1015–1017, and references therein.
- [11] For molecules containing more than two triorganoammonium iodide groupings see for instance: a) F. P. Schmidtchen, G. Müller, *J. Chem. Soc. Chem. Commun.* **1984**, 115–166; b) H. W. Schmalke, K. Hegtenschweiler, *Acta Crystallogr.* **1996**, C52, 1288–1293.
- [12] For the synthesis of Fréchet type aryl ether dendrons see for example: a) C. J. Hawker, J. M. J. Fréchet, *J. Am. Chem. Soc.* **1990**, 112, 7638–7647. For an analogous synthetic approach see: b) B. Hong, T. P. S. Thoms, H. J. Murfee, M. J. Lebrun, *Inorg. Chem.* **1997**, 36, 6146–6147.
- [13] CAChe Molecular Modeling package, Molecular Mechanics at the MM2 parameter level, Oxford Molecular Group, **1998**.
- [14] The solubility features of the dye–dendrimer assemblies point to a clear interaction between the MO anions and the polycationic dendrimers, particularly because of the relatively low ion-solvating efficiencies of the solvents CH_2Cl_2 and benzene with respect to polar solvents such as DMSO and H_2O .
- [15] Note that different cores are present in the dendrimer molecules **5–10**. This difference most probably has an influence on the mobility of the MO anions in the corresponding dye–dendrimers assemblies and, consequently, on their ^1H NMR spectroscopic features. Interestingly,

- for the cationic model derivative $[(C_6H_5CH_2)_2NMe_2]Br$, that does not contain internal cavities, a similar $\Delta\delta$ (namely from $\delta = 3.12$ to 3.02) for the NMe_2 group was noted as compared with dendrimers **5** and **6** upon exchange of the bromide for a MO anion. (A. W. Kleij, R. van de Coevering, R. J. M. Klein Gebbink, G. van Koten, unpublished results). This latter result suggests a similar proximity (ion pairing) between the MO anion and the cationic NMe_2 groups in these species.
- [16] Samples of the dendrimer species **5–8** and their MO-containing derivatives were prepared in an oxygen-free atmosphere with a concentration in the range of 1–5 mM in $CDCl_3$. T_1 and T_2 measurements were carried out on a Varian Inova 300 MHz NMR spectrometer using the implemented *dot1* and Carr–Purcell–Meiboom–Gill T_2 experiments.
- [17] a) A. D. Meltzer, D. A. Tirrell, A. A. Jones, P. T. Inglefield, D. M. Hedstrand, D. A. Tomalia, *J. Am. Chem. Soc.* **1992**, *25*, 4541–4548; b) A. M. Naylor, W. A. Goddard III, G. E. Kiefer, D. A. Tomalia, *J. Am. Chem. Soc.* **1989**, *111*, 2339–2341.
- [18] M. E. Piotti, F. Rivera, R. Bond, C. J. Hawker, J. M. J. Fréchet, *J. Am. Chem. Soc.* **1999**, *121*, 9471–9472.
- [19] The synthesis and full characterization of this compound will be reported elsewhere.

Received: May 2, 2000 [F2452]